

A Dynamic Codebook Design for Analog Beamforming in MIMO LEO Satellite Communications

Joan Palacios¹, Nuria González-Prelcic¹, Carlos Mosquera² and Takayuki Shimizu³

¹Electrical and Computing Engineering Department, North Carolina State University, Raleigh, NC, USA

²atlanTTic Research Center, Universidade de Vigo, Vigo, Spain

³Toyota Motor North America, Mountain View, CA, USA

Abstract—Beamforming gain is a key ingredient in the performance of LEO satellite communication systems to be integrated into cellular networks. However, beam codebooks previously designed in the context of MIMO communication for terrestrial networks, do not provide the appropriate performance in terms of inter-beam interference and gain stability as the satellite moves. In this paper, we propose a dynamic codebook that provides a stable gain during the period of time that the satellite covers a given cell, while avoiding link retraining and extra calculation as the satellite moves. In addition, the proposed codebook provides a higher signal-to-interference-plus-noise (SINR) ratio than those DFT codebooks commonly used in cellular systems.

I. INTRODUCTION

New flexible payloads are becoming more common in emerging satellite services due to significant innovations in active antennas and modular processing blocks, among others [1], [2]. These new technologies pave the way for the integration of satellite communications in general, and LEO constellations in particular, into future cellular networks. However, many open challenges still need to be addressed at the physical layer, including the design of appropriate beamforming strategies, modulation and coding schemes or approaches for link adaption [3].

To provide the required beamforming gain, analog fully reconfigurable beamforming networks entail high mass and power dissipation, limiting the number of beams. In the particular case of LEO satellites, large efforts are underway to develop hybrid arrays combining analog beamforming at a subarray level with digital processing of subarrays. Despite the expected performance, especially for large arrays, the flexibility comes at a cost, in such a way that the most relevant massive LEO constellations [4], [5] which are either operational or near to be, still make use of fixed analog beams. However, and similarly to terrestrial cellular systems, some degree of beam steering is desirable to focus the resources at will, keeping in mind that the size of satellite beams is much larger than that for terrestrial beams, able to offer better spatial discrimination.

Beam codebooks for cellular networks being deployed are based on an oversampled 2-D Discrete Fourier Transform (DFT) type grid of beams [6], [7]. This design was adapted in [8] to LEO systems by using the interpolation factor to adjust

the beamwidth to the size of the region of interest. However, as shown in [8], using this type of codebook results in a high signal-to-interference-plus-noise ratio (SINR) and a large variation in beamforming gain inside the beam switching time. In addition, the handovers between beams when using a static codebook are very frequent, degrading the user experience [9]. New designs that account for the mobility of the LEO satellite and the short amount of time that a given location is under the coverage of a LEO beam, need to be devised.

In this paper we address the problem of analog beamforming for LEO payloads with limited reconfigurability, by designing a family of codebooks that, together with the appropriate switching strategy, can steer the beams with limited resolution on the region to serve. The proposed design minimizes the number of handovers between beams for the ground terminal while keeping a stable beamforming gain during the period of time that the same LEO satellite is serving a given user.

II. SYSTEM MODEL

We consider the link between a LEO satellite and a user terminal operating in the Ku band with a bandwidth B and a full frequency reuse (FFR) scheme across beams. The user terminal is located in an elliptical region of interest (ROI) or coverage area with semi-radius R_x and R_y , designed following a given criteria, for example the one described in [8]. We denote with x the axis in the direction of the satellite's movement, while y is the axis orthogonal to x . The satellite is operating at a height h_{sat} with an associated angular speed of $w_{\text{sat}} = \frac{v_{\text{sat}}}{r_{\text{earth}} + h_{\text{sat}}}$, where R_{earth} is the Earth's radius and v_{sat} is the satellite linear speed. Note that the satellite linear speed also depends on the orbit height as

$$v_{\text{sat}} = \sqrt{G \frac{m_{\text{earth}}}{R_{\text{earth}} + h_{\text{sat}}}}, \quad (1)$$

where m_{earth} is the Earth's mass, and G is the gravitational constant. We also define the region of proximity (ROP) as the elliptical region of the same size as the ROI located right under the satellite. Note that the ROI and ROP do not have to be exactly the same, since the exact location of the ROI depends on the main directions of the beam patterns generated at the satellite.

The satellite is equipped with N_{RF} uniform planar sub-arrays of size $N_x^{\text{sub}} \times N_y^{\text{sub}}$, for a total number of antenna elements $N^{\text{sat}} = N_{\text{RF}} N_x^{\text{sub}} N_y^{\text{sub}}$. Note that while it is common to distribute the sub-arrays in a rectangular way, since each sub-array will be working independently of the others, their particular distribution will be irrelevant. By having the relative antenna elements positions defined by $\mathbf{k}_{\text{sat}} \in \mathbb{R}^{N^{\text{sat}} \times 3}$, with each of the radiating elements position at $[\mathbf{k}_{\text{sat}}]_{n,:}$, and denoting as $\mathcal{S}_2 = \{\mathbf{x} \in \mathbb{R}^3 \text{ s.t. } \|\mathbf{x}\| = 1\}$ the unitary sphere, the steering vectors that describe the response of the satellite's antenna in the direction $\mathbf{v} \in \mathcal{S}_2$ are denoted as $\mathbf{a}_{\text{sat}} : \mathcal{S}_2 \rightarrow \mathbb{C}^{N^{\text{sat}}}$ and defined as

$$[\mathbf{a}_{\text{sat}}(\mathbf{v})]_n = e^{-j \frac{2\pi}{\lambda} \langle [\mathbf{k}_{\text{sat}}]_{n,:}, \mathbf{v} \rangle}. \quad (2)$$

The LEO satellite serves a number N_u of mobile user terminals (UTs) on the ground by illuminating the ROI with N_b analog beams that are chosen from a given codebook and move with the satellite. We denote the analog precoding matrix used by the satellite as $\mathbf{F}_{\text{RF}} \in \mathbb{C}^{N^{\text{sat}} \times N_b}$. Given that the analog precoding stage will be implemented by means of a phase shifting network, we can write

$$[\mathbf{F}_{\text{RF}}]_{n,m} = \begin{cases} e^{j\phi_n} & \text{if } m = I_{\text{RF}}(n) \\ 0 & \text{otherwise,} \end{cases} \quad (3)$$

where $I_{\text{RF}}(n)$ is the index of the RF-chain to which the n -th antenna is connected. As in [10], we assume that the UTs exploit satellite's position information for beam tracking. We are considering a uniform planar array (UPA) of size $N^{\text{UT}} = N_x^{\text{UT}} \times N_y^{\text{UT}}$ at the terminals. The UT steering vector is denoted as $\mathbf{a}_u : \mathcal{S}_2 \rightarrow \mathbb{C}^{N_u}$, and is defined as $[\mathbf{a}_u(\mathbf{v})]_n = e^{-j \frac{2\pi}{\lambda} \langle [\mathbf{k}_u]_{n,:}, \mathbf{v} \rangle}$, where $\mathbf{k}_u \in \mathbb{C}^{N_u \times 3}$ are the antenna elements relative positions. The UT combiner is denoted as $\mathbf{w} \in \mathbb{C}^{N^{\text{UT}}}$, and is assumed to be analog-only.

We adopt a Rician geometric channel model with LoS complex gain γ and Rician factor K_r as in [8]. Given the steering vectors for the satellite and the UT previously defined, and assuming perfect symbol and carrier synchronization, the equivalent channel matrix is

$$\mathbf{H} = \gamma \left(\mathbf{a}_u \left(\frac{\mathbf{x}_u - \mathbf{x}_{\text{sat}}}{\|\mathbf{x}_u - \mathbf{x}_{\text{sat}}\|} \right) + \sqrt{\frac{1}{K_r}} \mathbf{a}_R \right) \mathbf{a}_{\text{sat}}^H \left(\frac{\mathbf{x}_{\text{sat}} - \mathbf{x}_u}{\|\mathbf{x}_{\text{sat}} - \mathbf{x}_u\|} \right) \quad (4)$$

where \mathbf{x}_{sat} is the satellite position, \mathbf{x}_u is the UT position, and $\mathbf{a}_R \sim \mathcal{CN}(0, \mathbf{\Sigma})$ is the Rician component satisfying $\text{trace}(\mathbf{\Sigma}) = \|\mathbf{a}_u \left(\frac{\mathbf{x}_u - \mathbf{x}_{\text{sat}}}{\|\mathbf{x}_u - \mathbf{x}_{\text{sat}}\|} \right)\|^2$. The term γ includes all path loss effects, dominated by the free space path loss $LP_{\text{fs}}[\text{dB}]$ and the atmospheric attenuation $LP_{\text{at}}[\text{dB}]$.

The signal-to-noise ratio (SNR) can be written in terms of the received signal strength (RSS) and the noise power σ^2 as [11]

$$\text{SNR}[\text{dB}] = \text{RSS}[\text{dBW}] - \sigma^2[\text{dBW}] \quad (5)$$

$$\begin{aligned} \text{RSS}[\text{dBW}] = & P_{\text{TX}}[\text{dBW}] - LP_{\text{cable}}[\text{dB}] + G_{\text{TX}}[\text{dB}] \\ & - LP_{\text{at}}[\text{dB}] - LP_{\text{fs}}[\text{dB}] + G_{\text{RX}}[\text{dB}] \end{aligned} \quad (6)$$

$$\sigma^2[\text{dBW}] = T[\text{dBK}] + k[\text{dBW/K/Hz}] + B[\text{dBHz}], \quad (7)$$

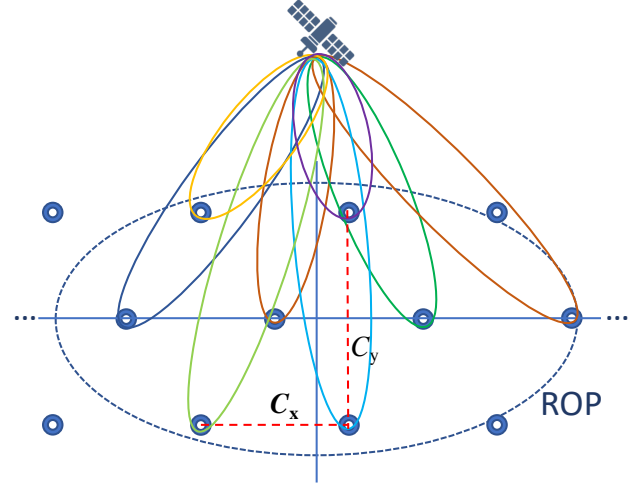


Fig. 1: Illustration of the idea behind the design of the initial codebook. The beams in the initial codebook are designed to have maximum gain at the points in the hexagonal lattice which fall inside the satellite's ROP.

where P_{TX} is the transmit power, G_{TX} is the transmit antenna gain, LP_{cable} is the cable loss between the antenna and the transmitter, and G_{RX} is the receiver antenna gain. Additionally, T and k denote the noise temperature and the Boltzmann constant, respectively. The receiver gain G_{TX} of this antenna when considering a Rician channel is extracted from [8] to be

$$G_{\text{RX}} = 10 \log_{10} \left(N_x^{\text{UT}} N_y^{\text{UT}} + \frac{1}{K_r} \right). \quad (8)$$

Same as in [8], we include the gain due to capturing the Rician component of the channel in the receiver as a natural result to ease the formulation.

III. DYNAMIC CODEBOOK DESIGN

Given a specific coverage area, our goal is to design a codebook of analog precoders that provides appropriate coverage, minimizing the SNR and SINR loss due to the satellite movement and the static beams. This loss has been described and numerically evaluated in [8] for a 2D DFT beam codebook as that used in 5G New Radio (NR). In this section, we design a set of feasible analog precoders that enable seamless communication without having to re-train the link every time a user is not covered anymore by a given beam due to the satellite's movement.

There are three main ideas behind our design: 1) selection of a basic codebook that provides a better SINR than that associated to the DFT codebook; 2) introduction of a codebook adaptation mechanism so the SNR variation due to the satellite movement is compensated; and 3) definition of a beam ID permutation protocol over the codebook that minimizes handovers. In the next paragraphs we describe these different components of the final design.

A. Initial codebook design

For the initial codebook design we choose to create beams whose maximum gains appear at the points of a given trian-

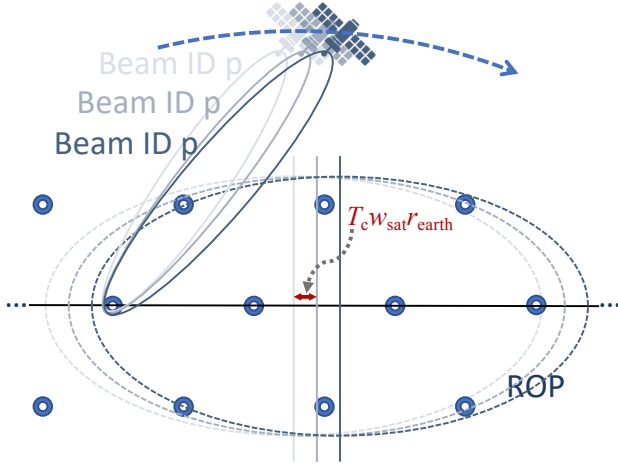


Fig. 2: Illustration of the idea behind the dynamic codebook. The beams in the codebook are redesigned every T_c to compensate for the satellite's movement. The number of active beams corresponds to the number of points in the triangular lattice that fall inside the satellite's ROP every time the beam codebook is updated.

gular (or hexagonal) lattice, as illustrated in Fig. 1. The points in the triangular lattice are scaled to be proportional to the diameter covered by a beam-width by a factor $C_x = \frac{\pi h_{\text{sat}}}{ON_{\text{sub}}}$ in the x direction and by a factor $C_y = \frac{\pi h_{\text{sat}}}{ON_{\text{sub}}}$ in the y direction, where O is defined as the oversampling factor. The value of the oversampling factor is chosen to adjust the number of points of the triangular lattice that will fall inside the satellite's shadow, i.e., the number of beams that will illuminate this region. The choice of a triangular lattice over a rectangular one (as that associated to a DFT codebook), gives rise to the common hexagonal tessellation in satellite footprints, and prevents the existence of locations with up to four beams with equal gain, highly detrimental for the signal-to-interference-plus-noise ratio (SINR). In addition, the alignment of the x-axis with the triangulation minimizes the periodicity interval of the lattice in that direction.

B. Codebook adaptation

The main idea behind our design consists of automatically updating the analog precoder every time interval of length T_c to compensate for the satellite's movement without the explicit need of computing a new precoder, but simply playing it from a dynamic codebook in a predefined order. This is illustrated in Fig. 2 for one of the beams in the initial codebook. This way, the beam pattern that points to a specific point in the triangular lattice is updated in a temporal grid to keep a high gain while that point is within the reach of the satellite's ROP. In an ideal system, the beam pattern would be adapted instantaneously as the satellite moves, but in a practical system only a periodic adaptation is feasible.

To simplify the dynamic codebook design problem, we adopt the geometry of the stereographic projection (ignoring the Earth's curvature and assuming the origin of coordinates is at the satellite's location), and using the unitary direction

of the satellite movement as x-axis and the perpendicular to the satellite movement and the orbital plan as the y-axis. The inaccuracies generated by this adoption can be neglected in the context of a LEO constellation, due to the high altitude of the satellites. Under this assumption, the condition of maximizing the stability of the directionality over the Earth's surface is equivalent to correcting the relative movement of the UT with respect to the satellite due to the satellite movement, i.e. $\mathbf{v}'_u = [-r_{\text{Earth}} w_{\text{sat}}, 0, 0]$. Note that during the time interval T_c the point of maximum directionality relative to the satellite moves a distance of $T_c r_{\text{Earth}} w_{\text{sat}}$ in the opposite direction to the satellite's movement. This tells us how to design the subsequent codebooks given an initial codebook.

Now we define the spatial shift in the x axis of the satellite's ROP over a period KT_c as $\Delta = KT_c w_{\text{sat}} r_{\text{Earth}}$ for a given integer number K . For an efficient implementation of the dynamic codebook, we realize that by setting T_c such that the scaling factor satisfies $C_x = \Delta$, the lattice becomes invariant to the spatial shift Δ . This means that by selecting an integer number K , we can create a cyclic dynamic codebook where each iteration lasts T_c , repeats every K iterations (cycle), and, as we will explain in Section III-C, shuffles indices for coherence. Mathematically, the lattice points of the k -th iteration can be expressed as

$$\begin{aligned} \mathcal{L}_k &= C_x \left(-\frac{k}{K} + \mathbb{Z} \right) \times \sqrt{3} C_y \mathbb{Z} \\ &\cup C_x \left(\frac{1}{2} - \frac{k}{K} + \mathbb{Z} \right) \times \sqrt{3} C_y \left(\frac{1}{2} + \mathbb{Z} \right), \\ T_c &= \frac{\pi h_{\text{sat}}}{K w_{\text{sat}} r_{\text{Earth}} O N_{\text{sub}}}. \end{aligned} \quad (9)$$

\mathcal{L}_k describes the lattice points assuming an infinite lattice, although for the definition of the final codebook we just need to keep those points that fall inside the coverage area. The condition for a point (x, y) being inside the elliptical ROI \mathcal{E} is $\left(\frac{x}{R_x} \right)^2 + \left(\frac{y}{R_y} \right)^2 \leq 1$. Thus, we select the points in \mathcal{L}_k that fulfill this equation. We do this for each iteration k , leading to a different number of points being inside the ellipse over time as k changes, and in consequence having a slightly different number of RF-chains and active beams in use over time. This process is illustrated in Fig. 3 for $K = 4$, i.e., a dynamic codebook built from 4 static codebooks in 4 iterations. The duration of the cycle is $4T_c$ in this case. Note that in each iteration, the number of active beams can decrease, increase, or keep unchanged, depending on the set of points of the triangular lattice that stay inside the corresponding ROP.

To compute the expression for the beamformers in the dynamic codebook as a function of the iteration k , by considering a point (x, y) at height 0 with origin on the satellite's shadow, the direction from the satellite to that point can be computed as $\frac{\mathbf{x}_u - \mathbf{x}_{\text{sat}}}{\|\mathbf{x}_u - \mathbf{x}_{\text{sat}}\|} = \frac{1}{\sqrt{x^2 + y^2 + h_{\text{sat}}^2}} (x, y, -h_{\text{sat}})$. Constructive interference to create a narrow beam-pattern in that direction can be achieved by setting the satellite's n -th antenna's phase-shift equal to the normalized satellite's steering vector coefficient evaluated at that direction, i.e., $[\mathbf{a}_{\text{sat}}^H \left(\frac{\mathbf{x}_{\text{sat}} - \mathbf{x}_u}{\|\mathbf{x}_{\text{sat}} - \mathbf{x}_u\|} \right)]_n / \sqrt{N_{\text{x}}^{\text{sub}} N_{\text{y}}^{\text{sub}}}$. Note that the normalization factor depends on the size of the subarray connected to a specific RF chain. In consequence, for every iteration k ,

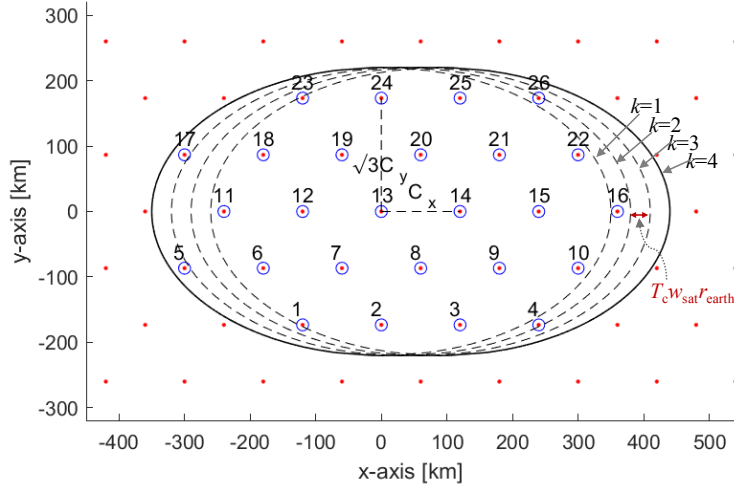


Fig. 3: Representation of the hexagonal lattice \mathcal{L}_k , for a toy example with $K = 4$. The points of the hexagonal lattice are marked in red. Each ellipse represents the ROP for different time lapses. The beams IDs are updated so there is no need of handover at the user terminal, which always sees the same ID over the time the same LEO satellite is illuminating the cell. The subset of points that are or will be active in any of the lattice translations are circled in blue, and labeled following the proposed criteria.

with one RF-chain per beam pointing to $(x_m, y_m) \in \mathcal{L}_k \cap \mathcal{E}$, we can set the phase-shift coefficient of the n -th antenna connected to that RF-chain to

$$[\mathbf{F}_{\text{RF},k}]_{n,m} = \frac{e^{-j\pi \frac{1}{\sqrt{x_m^2 + y_m^2 + h_{\text{sat}}^2}} (x_m[\mathbf{k}]_{n,1} + y_m[\mathbf{k}]_{n,2})}}{\sqrt{N_x^{\text{sub}} N_y^{\text{sub}}}}, \quad (10)$$

for $I_{\text{RF}}(n) = m$, and 0 otherwise.

C. Beam IDs permutations

Beam IDs are permuted at each iteration if the dynamic codebook to guarantee that the beam ID covering a given hexagonal area is static, as illustrated in Fig. 2. In terms of the directionality of the beam-pattern, this means that the point on the Earth's surface such that a specific beam with ID m at time t has its maximum directionality, is also the maximum directionality point for the beam with ID m at time $t + nT_c, n \in \mathbb{Z}$.

After completion of a cycle of the codebook, and due to the satellite movement, the Earth location initially illuminated by the beam pointing to the lattice point $(x, y) \in \mathcal{L}_k$, becomes illuminated by the beam pointing to the lattice point $(x - \frac{\pi h_{\text{sat}}}{o N_x^{\text{sub}}}, y) \in \mathcal{L}_k$, so that the beam index changes. To avoid the need of constant handover, a permutation of the beam indices can be applied under the constraint that if $\{(x, y), (x - \frac{\pi h_{\text{sat}}}{o N_x^{\text{sub}}}, y)\} \in \mathcal{L}_k \cap \mathcal{E}$, then the index of the beam pointing to the lattice point (x, y) gets updated to the index of the beam pointing to the lattice point $(x - \frac{\pi h_{\text{sat}}}{o N_x^{\text{sub}}}, y)$. A proposal to address the index updating procedure starts by determining all the lattice points that will be eventually active: $\{(x, y) \in \mathcal{L}_0 \text{ such that } (x - \frac{k\pi h_{\text{sat}}}{K o N_x^{\text{sub}}}, y) \in \mathcal{E} \text{ for } 0 \leq k < K\}$, then label them as (x_i, y_i) for the i th point, such that $y_i < y_k$

or $x_i < x_j$ if $y_i = y_j$ with respect to the coordinates (x_j, y_j) of point j if $i < j$. With this, the updating procedure boils down to a cyclic increase of each beam index in one unit.

Note that when using this codebook, the cells on the Earth surface, considered as those locations receiving higher power from a given beam, will be nearly hexagonal, with sides at the equidistant lines to the six nearest lattice points as will be shown in the simulations.

Parameter	Symbol	Value	Units
<i>Constellation and ROI</i>			
Satellite height	h_{sat}	1300	km
Number of orbital planes	N_p	83	
Number of satellites per orbital plane	N_s	53	
Orbital plane inclination	θ_{op}	53	degrees
Semiradius of the ROI in x -dimension	R_x	534.1	km
Semiradius of the ROI in y -dimension	R_y	170.5	km
<i>Channel</i>			
Carrier frequency	f_{DL}	11.45	GHz
Bandwidth	B_{DL}	250	MHz
Atmospheric path loss	LP_{at}	0.017	dB
Rician factor	K_r	10	
<i>Satellite</i>			
Sub-array elements in x -dimension	N_x^{sub}	12	
Sub-array elements in y -dimension	N_y^{sub}	24	
Number of RF chains	N^{RF}	13	
Transmit power	P_{TX}	15	dBW
Oversampling factor	o	1.4	
<i>User terminal</i>			
User antenna gain	G_{RX}	27.6	dB
Receiver noise temperature	T	24.1	dB

TABLE I: System parameters for the simulation of the downlink of a LEO SatCom system operating in the Ku band.

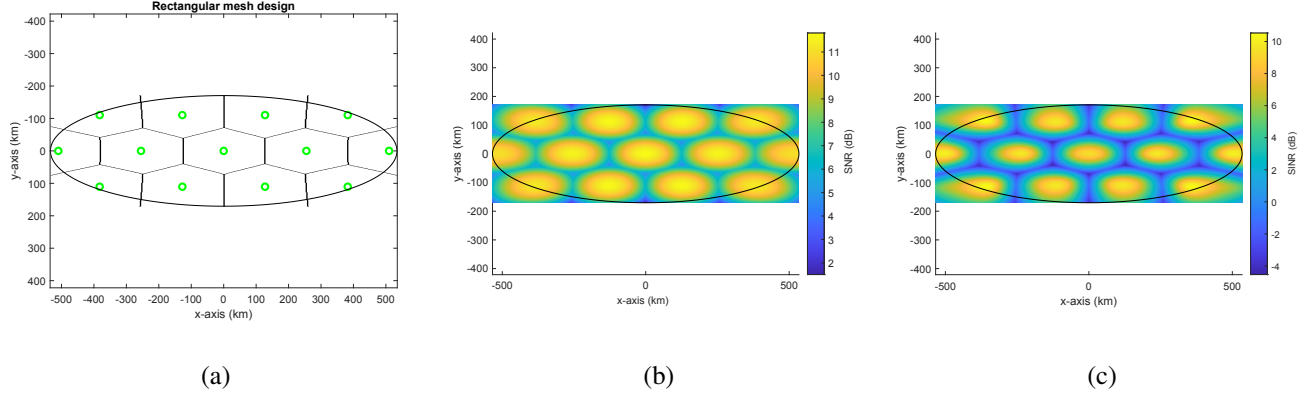


Fig. 4: (a) Cells associated to the different beams; points marked in green show the location where the beam gain is maximum. (b) SNR when using the best beam for each cell. (c) SINR when using the best beam for each cell.

IV. SIMULATION RESULTS

We simulate the downlink of a LEO satellite communication system operating with the parameters described in Table I. The LEO constellation includes 53 satellites in each of its 83 orbits, with an orbital plane inclination of 53° . Each satellite orbits at a 1300 km height, covering an ellipsoidal area with semi-radius 534.1 km in the x axis and 170.5 km in the y axis. The satellite large phased array consists of 13 sub-arrays of 12×24 antennas, which operate independently. The gain at the UT corresponds to that of a uniform rectangular array of 24×24 elements, i.e., $G_{RX} = 27.6\text{dB}$.

We start by analyzing the satellite's coverage in the elliptical area when using a static initial codebook as described in Section III-A. To this end, since LP_{fs} , G_{TX} and G_{TX}^{interf} are user location dependent, we plot maps of the SNR and SINR in Fig. 4. The values of the SNR and SINR for each location have been computed using (15) and (19) in [8]. While the SNR values show relatively small variations all over the ellipse, the SINR map shows areas with relative high interference. This is a consequence of using the same codebook on a single satellite for all users over the whole bandwidth spectrum. A full frequency reuse leads to SINR values no larger than -3 dB at those locations covered by three beams with the same gain. We compare now the performance provided by this initial codebook design with that of an oversampled 2D DFT codebook comprised of 15 beam-patterns, evaluated in [8] in the context of a LEO satellite communication system. To that aim, we evaluate the probability of the SINR being larger than a given threshold. Fig. 5 shows that our design significantly outperforms the 2D DFT codebook used in 5G NR even when using fewer beam-patterns to cover the same area, providing a higher probability of achieving a given SINR threshold. For example, the probability of having a SINR larger than 4 dB is 0.5 when using the proposed dynamic codebook, and only 0.25 when operating with a fixed 2D DFT codebook. These results show how the initial codebook design proposed in Section III-A outperforms the 2D DFT codebook. Now we evaluate

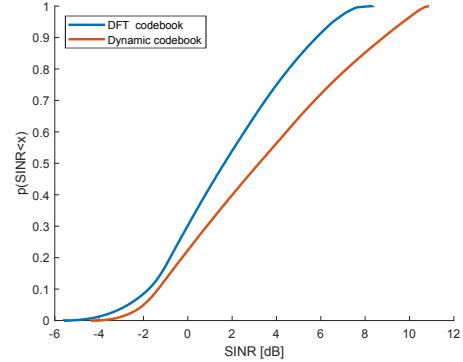


Fig. 5: SINR cumulative distribution function for a DFT based approach defined in [8] and the proposed dynamic codebook. The hexagonal lattice considered in our initial codebook design introduces a gain in SINR with respect to the rectangular lattice inherent to the 2D-DFT codebook.

the performance of the dynamic codebook design based on the previous initial codebook. To this aim, we compute the SNR degradation over time due to the satellite's movement. The UT is initially located at the center of the ROP, which is moving as the satellite travels. Fig. 6 shows the evolution of the SNR value when using the initial codebook without beam adaptation, and the proposed dynamic codebook. When using the initial codebook in a static way, we can see that the user is illuminated for around 30 seconds by each beam-pattern, with an SNR variation of around 3dB inside the beam footprint. In addition, there is a progressive degradation of the peak gain that the best beam can provide. With the proposed dynamic codebook, the UT experiences an SNR with a variation of the order of only 0.5 dB over the same period of time. We consider now the evolution of SNR over time for a user located 50 km away on the y-axis from the center of the ROP, using both the DFT codebook and the dynamic codebook. The results are shown in Fig. 7. In this case, the user experiences a variation of 1.5 dB with the static 2D DFT codebook, while the dynamic codebook provides approximately the same peak SNR over the

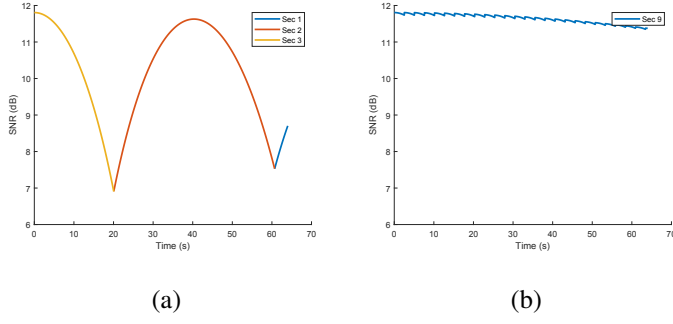


Fig. 6: Time SNR variation due to the satellite movement: (a) using the DFT codebook in [8]; (b) proposed dynamic codebook.

analyzed cycles. These two examples show how the dynamic codebook clearly outperforms the static DFT codebook at different user locations.

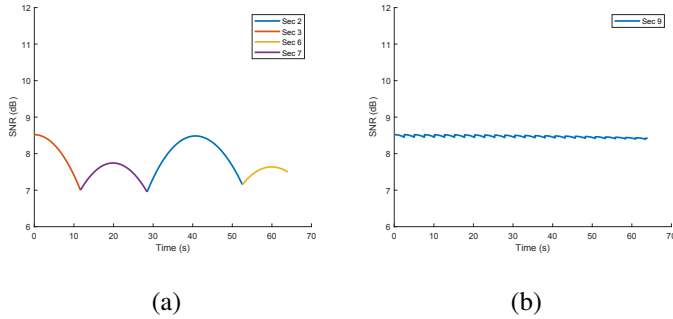


Fig. 7: Time SNR variation due to the satellite movement for a user located 50 km away on the y-axis from the center of the ROP : (a) using the DFT codebook in [8]; (b) proposed dynamic codebook.

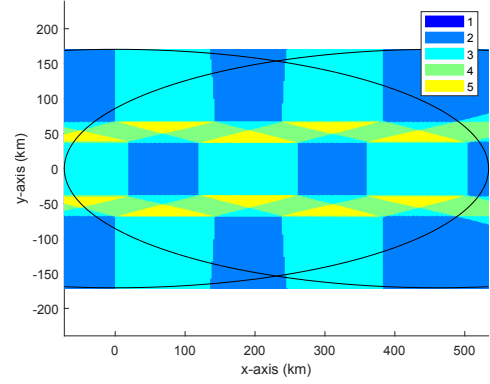
Finally, we evaluate the ability of the beam ID permutation mechanism to reduce the number of handovers. Fig. 8 shows the number of handovers that a user located at a given point would experience when using the static and dynamic codebooks. It is easy to check that the number of handovers is kept to one for most of the locations in the ROI when using the dynamic codebook, while the static one requires at least three handovers for most of the locations.

V. CONCLUSIONS

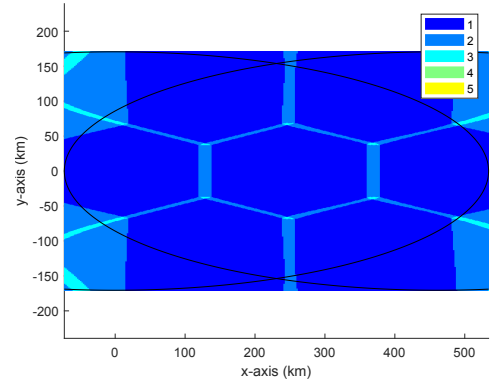
In this paper we have proposed a family of codebooks specifically designed for analog beamforming in LEO satellites, which affords some flexibility for beam steering without incurring in extra computational complexity at the payload. The selection of the appropriate codebook from a judiciously designed family allows to offer a smoother coverage to the ground terminals, minimizing handovers while keeping a stable beamforming gain.

REFERENCES

- [1] R. De Gaudenzi, P. Angeletti, D. Petrolati, and E. Re, "Future technologies for very high throughput satellite systems," *Intl. Journal of Satellite Communications and Networking*, vol. 38, no. 2, pp. 141–161, 2020.
- [2] P. Angeletti and R. De Gaudenzi, "A Pragmatic Approach to Massive MIMO for Broadband Communication Satellites," *IEEE Access*, vol. 8, pp. 132 212–132 236, 2020.



(a)



(b)

Fig. 8: Number of handovers experienced by a user at a given location: (a) using the initial codebook in a static way; (b) using the proposed dynamic codebook.

- [3] O. Kotheli, A. Guidotti, and A. Vanelli-Coralli, "Integration of Satellites in 5G through LEO Constellations," in *GLOBECOM 2017 - 2017 IEEE Global Communications Conference*, 2017, pp. 1–6.
- [4] I. del Portillo, B. G. Cameron, and E. F. Crawley, "A technical comparison of three low earth orbit satellite constellation systems to provide global broadband," *Acta Astronautica*, vol. 159, pp. 123–135, 2019.
- [5] S. Xia, Q. Jiang, C. Zou, and G. Li, "Beam Coverage Comparison of LEO Satellite Systems Based on User Diversification," *IEEE Access*, vol. 7, pp. 181 656–181 667, 2019.
- [6] H. Miao, M. D. Mueck, and M. Faerber, "Amplitude Quantization for Type-2 Codebook Based CSI Feedback in New Radio System," in *European Conf. on Networks and Communications (EuCNC)*, 2018, pp. 1–9.
- [7] Samsung, "WF on Type I and II CSI codebooks," 3GPP, Hangzhou, China, Tech. Rep. Meeting RAN1#89, May 2017.
- [8] J. Palacios, N. Gonzalez-Prelcic, C. Mosquera, T. Shimizu, and C. H. Wang, "A hybrid beamforming design for massive MIMO LEO satellite communications," *Frontiers in Space Technologies*, vol. 2, p. 4, 2021.
- [9] Y. Su, Y. Liu, Y. Zhou, J. Yuan, H. Cao, and J. Shi, "Broadband LEO Satellite Communications: Architectures and Key Technologies," *IEEE Wireless Communications*, vol. 26, no. 2, pp. 55–61, 2019.
- [10] J. Kim, M. Y. Yun, D. You, and M. Lee, "Beam Management for 5G Satellite Systems Based on NR," in *International Conference on Information Networking (ICOIN)*, 2020, pp. 32–34.
- [11] Technical Specification Group Radio Access Network, "Solutions for NR to support non-terrestrial networks (NTN) (Release 16)," 3GPP, Tech. Rep. V16.0.0, dec 2019.